Pheophorbide Derivatives Isolated from Açaí Berries (*Euterpea oleracea*) Activate an Antioxidant Response Element *In Vitro*

Suneel K. Kandagatla[a], **Robin Tate Uhl**[a], **Tyler N. Graf**[a], **Nicholas H. Oberlies**[a], **Gregory M. Raner**[b]

[a]Department of Chemistry and Biochemistry, The University of North Carolina at Greensboro, Greensboro, NC 27402

[b]Department of Biology and Chemistry, Liberty University, Lynchburg, VA 24515

Abstract

Activity-guided fractionation was used to isolate and identify two components of the Brazilian açaí berry (*Euterpe oleracea* Mart.) with the ability to induce antioxidant response element (ARE)-dependent gene transcription in human hepatoma (HepG2) cells. Using an ARE-Luciferase reporter construct in cultured HepG2 cells, a suite of fractions from dried and powdered açaí berries were evaluated for transcriptional up-regulation of the luciferase gene. Active fractions were further refined until several pure compounds were isolated and identified. These compounds belong to the pheophorbide class of molecules, and are composed of the methyl and ethyl esters of the parent pheophorbide A, all of which are classified as photosensitizers. Using standard pheophorbides, dose response studies were carried out, and ARE-activation could be observed at concentrations as low as 8.2 μM and 16.9 μM for pheophorbide A methyl ester and pheophorbide A, respectively. These studies not only suggest a possible source of antioxidant properties for the açaí berry, but may also explain the recently identified photosensitizing abilities of açaí products as well.

Keywords

Euterpe oleracea Mart; açaí; Nrf2; anti-oxidant; pheophorbide

---

The açaí [*Euterpe oleracea* Mart. (Arecaceae)] berry has become very popular in recent years as a functional food resulting from its health promoting effects, and in particular, its ability to reduce oxidative stress. Although açaí products have been shown to act effectively as an antioxidant *in vitro* and *in vivo*, it has not been well-characterized with regard to the mechanisms associated with these effects in humans [1]. Studies have demonstrated certain types of antioxidant effects in a variety of model systems [2,3] and whole organisms [4,5] that are consistent with the Nrf2-dependent mode of action. In addition, Monge-Fuentes *et al.* [6] demonstrated that formulations containing açaí oil were effective photosensitizers when applied to B16F10 melanoma cells and in tumor bearing C57BL/6 mice, indicating certain compounds in the berry may be effective in photodynamic therapy for melanoma.

graner@liberty.edu.

This is attributed to production of singlet oxygen, which has been shown to stimulate Nrf2-dependent pathways. Other studies in mice have shown that açaí products reduce lipid peroxidation [7], increase antioxidant gene expression [8], and protect against carcinogen induced oxidative stress [9].

Açaí extract can reduce oxidative stress induced by cigarette smoke in mice, which could also be partially due to activation of anti-oxidant gene expression. In addition, human trials have indicated efficacy in reducing pain and inflammation, along with improvements in range of motion, all of which were highly correlated to antioxidant status [10,11]. Furthermore, chemical analysis of the freeze dried açaí [12] has indicated the presence of several types of polyphenolic compounds with known antioxidant properties, including anthocyanins and flavones [3]. Schauss *et al.* [12] reported the pulp of açaí juice to contain high levels of anthocyanins and other classes of polyphenolic compounds, and according to Milbury *et al.* [13], the bioavailability of these compounds may be sufficient to effect biological targets.

The luciferase reporter used in the study, pGL3-*wt*ARE, was constructed according to methods reported by Kim et al. [14] using the pGL3 luciferase vector (Figure 1). This vector incorporates a functional Antioxidant response element (ARE) in front of an active promoter controlling luciferase gene expression. Thus, Nrf2 activators will induce luciferase expression and activity in the cultured cells. A second construct in which the ARE sequence was mutated (pGL3-mARE) was also produced as a negative control. The data shown in Figure 2 demonstrate that luciferase activity was substantially induced at 100 μM tBHQ using the *wt*ARE construct, while pGL3 and pGL3-mARE were unresponsive to the inducer. Furthermore, the açaí chloroform extract at 200 μg/mL produced an inductive effect that was even more pronounced than tBHQ, suggesting the presence of ARE inducers in this extract. Induction by the butanol, aqueous and hexane extracts, at the same concentration, were less than 1.5-fold. It should be noted that the level of induction by the positive control, tBHQ, varied from experiment to experiment, however, it generally fell within the range of 2.5- to 5-fold.

The bioactivity-guided fractionation approach was then followed using the chloroform extract in an attempt to identify components in this fraction with the ability to activate the ARE-luciferase reporter system in the HepG2 cells. Figure 3 represents the scheme used to track active fractions through each generation of purification. The chloroform extract was fractionated into 10 sub-fractions designated 34–1 through 34–10. Each fraction was assessed for its ability to activate the reporter plasmid in HepG2 cells at a concentration of 50 μg/mL; this concentration was chosen based on previous experience working on the bioactivity-directed fractionation of herbals [15–17]. Fractions highlighted by the vertical shading represent those fractions that were carried forward in the purification based on activity and yield. Since fraction 34–8 resulted in the most significant activation, it was subsequently fractionated into 8 sub-fractions designated as 38–1 through 38–8. Sub-fractions 38–1 through 38–4 displayed modest induction at 50 μg/mL, however, potent induction was not observed for any of these sub-fractions. These sub-fractions were therefore fractionated further producing the 61-series, the 62-series, the 63-series, and the 64-series, all indicated by the vertical hashed shading. The 38–8 fraction (checkered shading

in Figure 3) actually produced a significant response in the reporter assay, however, due to paucity of sample further purification was not pursued. Importantly, multiple criteria were used at each stage to select fractions to carry forward in the process. In addition to activity in the luciferase assay, the total mass of material in the fraction was an important consideration in the fractionation approach, along with the chromatographic complexity of the samples at later stages of the process. For example, although the fraction 64–1 (shown as checkered shading) was very active, the amount of material found in this fraction was very low, and subsequent purification was not feasible.

Following this approach to completion, fractions 97-B and 97-D were shown to contain single active compounds (Figure 4). Fraction 97-B (3.3 mg) was identified as pheophorbide A methyl ester using high resolution mass spectrometry with obsd. m/z 607.2917 [M+H]$^+$ (calcd. for $C_{36}H_{39}N_4O_5$, 607.2915) and comparison to literature NMR data [18]. Fraction 97-D (2.7 mg) was identified as pheophorbide A ethyl ester using high resolution mass spectrometry with obsd. m/z 621.3074 [M+H]$^+$ (calcd. for $C_{37}H_{41}N_4O_5$, 621.3071), and comparison to literature NMR data [19].

Finally, pure standards of pheophorbide a (the parent compound) and pheophorbide a methyl ester were obtained commercially, and a dose response was generated for each using the ARE-driven luciferase reporter. As shown in Figure 5, both compounds resulted in increased luciferase expression at concentrations as low as 8.2 μM, and there was a clear dose-dependent increase observed for each.

Pheophorbides are known plant products related to the chlorophyll molecule and have been shown to have interesting medical properties and applications. For example, a major application of these photoactive compounds is in photodynamic therapy [20]. Indeed, Monge-Fuentes *et al*. [6] demonstrated both in cultured cells and in tumor induced mice that açaí berry oil possess compounds with photosensitizing properties, which may be useful for photodynamic therapy. Furthermore, Liu *et al*. [21] have shown the parent compound isolated from the açaí berry, pheophorbide A, reduces proliferation and metastasis of human prostate cancer cells in vitro when used as a photodynamic agent. In addition, Hagiya *et al*. [22] demonstrated that pheophorbides could induce Nrf2-dependent gene expression, consistent with our findings in HepG2 cells.

Due to the light sensitive nature of the compounds, all treatments were carried out under black light. That induction of the luciferase reporter was observed in a dose dependent manner in the absence of light suggests that the pheophorbides possess some direct activating effects on the Nrf2-dependent anti-oxidant pathway, however, additional experiments to evaluate the effects of light on this induction would help to clarify the mechanisms involved.

In summary, we have demonstrated the effective use of bioactivity-guided fractionation for the isolation and identification of individual constituents of the Brazilian açaí berry with potential antioxidant properties related to their ability to stimulate ARE-dependent gene induction. Identification of these active compounds as photosensitizers suggests alternative therapeutic applications for this versatile natural product.

Experimental

Açaí berry freeze dried extracts

Freeze dried powdered açaí berry was purchased from Optimally Organic Inc, (Westlake Village, CA); all of the material was from a single lot, and a voucher specimen was deposited in the Herbarium of the University of North Carolina at Chapel Hill (NCU601336). Moreover, a sample of the berry powder was submitted for genetic analysis to Authentechnologies Inc, (Richmond, CA), which showed the most likely identity of the sample to be *Euterpe oleracea* (Açaí), based on comparison with authentic samples and divergence from all closely related species analyzed.

Construction of the antioxidant reporter vector

The firefly luciferase reporter plasmid pGL3 was purchased from Promega and was genetically engineered to include a known ARE sequence that is present in the human thioredoxin promoter. Standard cloning techniques were employed to produce the corresponding pGL3-ARE vector described by Kim *et al.* [14] which has been used effectively to monitor ARE induction in a variety of human cell lines, including HepG2.

Induction of ARE-reporter in HepG2 cells

Expression of luciferase was determined using a commercial Dual-Glo® Luciferase Assay System from Promega according to the established protocols and a BMG Labtech PolarStar Optima 96 well plate reader for luminescence measurements. HepG2 cells were obtained from ATCC and have been grown and maintained in Dulbecco's modified Eagle medium, high (4.5 g/L) glucose, 4.0 mM glutamine and 1.0 mM sodium pyruvate [21]. For all subsequent experiments, cells were cultured and grown to 60% confluence and transfected with the pGL3-ARE reporter plasmid using FuGene® reagent for 24 hours. Cells were treated with extract or pure compounds for 24 hours. The activities of luciferase expressed in HepG2 cells were normalized by co-transfecting HepG2 cells with pRL-TK Renilla reporter vector as an internal control. All cell culture experiments were carried out in triplicate, and independently reproduced. Positive control experiments were also carried out in parallel in which *tertiary* butylhydroquinine (tBHQ), at 100 μM, was used to induce luciferase activity in the pGL3-ARE containing cells. Active fractions were identified as those inducing a minimum of 2x luciferase activity relative to the negative control.

Preparation of extracts

For the initial fractionation, 1820 g of freeze dried açaí powder was extracted in 4L MeOH, by stirring at room temperature, to generate a methanol extract (Figure 2). The methanol fraction was filtered and the volume reduced to 2L and subsequently partitioned with 9:1:10 MeOH:H_2O:hexane in a total volume of 4L. Aqueous MeOH is immiscible with hexane, which allows for the "defatting" of the original MeOH extract, thereby generating a hexane fraction (**1**) containing 62.5 g dried material (Figure 2). The aqueous MeOH fraction was dried and partitioned with 4:1:5 chloroform:MeOH:H_2O in a total volume of 4L. The organic layer produced 18.0 g of dried chloroform extract (**2**). Finally, the remaining aqueous fraction was partially evaporated to remove methanol and partitioned between equal

volumes of n-BuOH and H_2O (total volume 4L) resulting in 29.6 g and 78.1 g of dried butanol (**3**) and aqueous (**4**) fractions, respectively.

Total fractionation protocol through the 97 series

34 series—The chloroform extract (18 g) was adsorbed onto celite and chromatographed on a 330-gram silica column utilizing a Combiflash Rf 200 automated flash chromatography system (Teledyne-Isco, Lincoln, NE). A gradient from 100 % n-hexanes to 100 % chloroform then to 100 % MeOH was used over 28 column volumes to obtain 10 fractions labeled the 34 series.

38 series—Fraction eight of the 34 series (34–8, 6.14 g) was adsorbed onto celite and chromatographed on a 120-gram "gold" (high performance) silica column utilizing a Combiflash Rf 200. A gradient from 100 % n-hexanes to 100 % acetone then to 100 % MeOH was used over 18 column volumes to obtain 8 fractions hereby labeled the 38 series.

61 series—Fraction one of the 38 series (38–1, 2.00 g) was adsorbed onto celite and chromatographed on a 30-gram diol column utilizing a Combiflash Rf 200. A gradient from 100 % n-hexanes to 100 % ethyl acetate then to 20 % methanol was used over 22 column volumes to obtain 7 fractions hereby labeled the 61 series.

62 series—Fraction two of the 38 series (38–2, 1.18 g) was adsorbed onto celite and chromatographed on a 30-gram diol column utilizing a Combiflash Rf 200. A gradient from 100 % n-hexanes to 100 % ethyl acetate then to 20 % methanol was used over 22 column volumes to obtain 5 fractions hereby labeled the 62 series.

63 series—Fraction three of the 38 series (38–3, 0.96 g) was adsorbed onto celite and chromatographed on a 30-gram diol column utilizing a Combiflash Rf 200. A gradient from 100 % n-hexanes to 100 % ethyl acetate then to 20 % methanol was used over 24 column volumes to obtain 6 fractions labeled the 63 series.

64 series—Fraction four of the 38 series (38–4, 0.73 g) was adsorbed onto celite and chromatographed on a 30-gram diol column utilizing a Combiflash Rf 200. A gradient from 100 % n-hexanes to 100 % ethyl acetate then to 100 % methanol was used over 26 column volumes to obtain 5 fractions labeled the 64 series.

78 series—Fraction two of the 62 series (62–2, 739 mg) was chromatographed on a Gemini-NX C18 reverse phase HPLC column (250 × 21.2 mm) utilizing a ProStar preparative HPLC system (Varian Inc., Palo Alto, CA) running at 21.2 mL/min. A gradient from 50:50 to 100:0 acetonitrile:water was used over 50 min to obtain 9 fractions labeled the 78 series.

97 series—Fraction nine of the 78 series (78–9, 64.7 mg) was chromatographed on a Gemini-NX C18 reverse phase HPLC column (250 × 21.2 mm) utilizing a ProStar preparative HPLC system running at 21.2 mL/min. A gradient from 70:30 to 100:0 acetonitrile:water over 15 min followed by isocratic elution at 100:0 for 15 min to obtain 9 fractions labeled the 97 series.

MS and NMR characterization—High resolution electrospray ionization mass spectrometry (HRESIMS) data were collected using an electrospray ionization source coupled to a Q Exactive Plus system (Thermo Fisher Scientific, San Jose, CA) in positive ionization mode via a liquid chromatography/autosampler system comprised of an Acquity UPLC system (Waters Corp., Milford, MA).

The NMR data were collected using a JEOL ECS-400 spectrometer (JEOL USA, Inc., Peabody, MA) operating at 400 MHz for ^{1}H and 100 MHz for ^{13}C, and equipped with JEOL normal geometry broadband Royal probe.

Acknowledgments

References

[1]. Hu J, Zhao J, Khan SI, Liu Q, Liu Y, Ali Z, Li XC, Zhang SH, Cai X, Huang HY, Wang W, Khan IA (2014) Antioxidant neolignan and phenolic glucosides from the fruit of *Euterpe oleracea*. Fitoterapia, 99, 178–183. [PubMed: 25284430]

[2]. Zhou J, Zhang J, Wang C, Qu S, Zhu Y, Yang Z, Wang L. (2018) Açaí (Euterpe oleracea Mart.) attenuates alcohol-induced liver injury in rats by alleviating oxidative stress and inflammatory response. Experimental and Therapeutic Medicine, 15, 166–172. [PubMed: 29399060]

[3]. Xie C, Kang J, Li Z, Schauss AG, Badger TM, Nagarajan S, Wu T, Wu X. (2012) The açaí flavonoid velutin is a potent anti-inflammatory agent: blockade of LPS-mediated TNF-α and IL-6 production through inhibiting NF-κB activation and MAPK pathway. Journal of Nutritional Biochemistry, 23, 1184–91.

[4]. Guerra JF, Magalhães C, Costa DC, Silva ME, Pedrosa ML. (2011) Dietary açaí modulates ROS production by neutrophils and gene expression of liver antioxidant enzymes in rats. Journal of Clinical Biochemistry and Nutrition, 49, 188–194. [PubMed: 22128218]

[5]. Choi YJ, Choi YJ, Kim N, Nam RH, Lee S, Lee HS, Lee HN, Surh YJ, Lee DH. (2017) Açaí Berries Inhibit Colon Tumorigenesis in Azoxymethane/Dextran Sulfate Sodium-Treated Mice. Gut and Liver, 11, 243–252. [PubMed: 27965474]

[6]. Monge-Fuentes V, Muehlmann LA, Longo JP, Silva JR, Fascineli ML, de Souza P, Faria F, Degterev IA, Rodriguez A, Carneiro FP, Lucci CM, Escobar P, Amorim RF, Azevedo RB. (2018) Photodynamic therapy mediated by açaí oil (Euterpe oleracea Martius) in nanoemulsion: A potential treatment for melanoma. Journal of Photochemistry and Photobiology B, 166, 301–310.

[7]. Xie C, Kang J, Burris R, Ferguson ME, Schauss AG, Nagarajan S, Wu X. (2011) Açaí juice attenuates atherosclerosis in ApoE deficient mice through antioxidant and anti-inflammatory activities. Atherosclerosis, 216, 327–333. [PubMed: 21411096]

[8]. de Moura RS, Ferreira TS, Lopes AA, Pires K., Nesi RT, Resende AC, Souza PJ, da Silva AJ, Borges RM, Porto LC, Valenca SS. (2012) Effects of Euterpe oleracea Mart. (AÇAÍ) extract in acute lung inflammation induced by cigarette smoke in the mouse. Phytomedicine, 19, 262–269. [PubMed: 22138278]

[9]. Alessandra-Perini J, Perini JA, Rodrigues-Baptista KC, de Moura RS, Junior AP, dos Santos TA, Souza PJC, Nasciutti LE, Machado DE. (2018) Euterpe Olaracea extract inhibits tumorigenesis effect of the chemical carcinogen DMBA in breast experimental cancer. BMC Complementary and Alternative Medicine, 18, 116. doi: 10.1186/s12906-018-2183-z. [PubMed: 29609579]

[10]. Jensen GS, Ager DM, Redman KA, Mitzner M A, Benson KF, Schauss AG. (2011) Pain reduction and improvement in range of motion after daily consumption of an açai (Euterpe oleracea Mart.) pulp-fortified polyphenolic-rich fruit and berry juice blend. Journal of Medicinal Foods, 14, 702–711.

[11]. Udani JK, Singh BB, Singh VJ, Barrett ML. (2011) Effects of Açai (Euterpe oleracea Mart.) berry preparation on metabolic parameters in a healthy overweight population: a pilot study. Nutrition Journal, 10, 1–7. [PubMed: 21208446]

[12]. Schauss AG, Wu X, Prior RL, Ou B, Patel D, Huang D, Kababick JP. (2006) Phytochemical and nutrient composition of the freeze-dried amazonian palm berry, Euterpe oleraceae mart. (Açaí). Journal of Agricultural Food Chemistry, 54, 8598–603. [PubMed: 17061839]

[13]. Milbury PE, Vita JA, Blumberg JB. (2010) Anthocyanins are bioavailable in humans following an acute dose of cranberry juice. Journal of Nutrition, 140, 1099–1104.

[14]. Kim YC, Masutani H, Yamaguchi Y, Itoh K, Yamamoto M, Yodoi J. (2001) Hemin-induced activation of the thioredoxin gene by Nrf2. A differential regulation of the antioxidant responsive element by a switch of its binding factors. Journal of Biological Chemistry, 276, 18399–18406. [PubMed: 11279008]

[15]. Ngo N, Yan Z, Graf TN, Carrizosa DR, Kashuba AD, Dees EC, Oberlies NH, Paine MF. (2009) Identification of a cranberry juice product that inhibits enteric CYP3A-mediated first-pass metabolism in humans. Drug Metabolism and Disposition, 37, 514–522. [PubMed: 19114462]

[16]. Kim E, Sy-Cordero A, Graf TN, Brantley SJ, Paine MF, Oberlies NH. (2011) Isolation and identification of intestinal CYP3A inhibitors from cranberry (Vaccinium macrocarpon) using human intestinal microsomes. Planta Medica, 77, 265–270. [PubMed: 20717876]

[17]. Won CS, Oberlies NH, Paine MF. (2012) Mechanisms underlying food-drug interactions: Inhibition of intestinal metabolism and transport. Pharmacology & Therapeutics, 136, 186–201. [PubMed: 22884524]

[18]. Schwikkard SS, Mulholland DA, Hutchings A. (1998) Pheophytins from *Tapura Fischeri*. Phytochemistry 9, 2391–2394.

[19]. Jin PF, Deng ZW, Pei YH, Lin WH. (2005) Two pheophytin type analogues from marine sponge *dysidea sp*. Chinese Chemical Letters, 16, 209–211.

[20]. Rapozzi V, Miculan M, Xodo LE, (2009) Evidence that photoactivated pheophorbide a causes in human cancer cells a photodynamic effect involving lipid peroxidation. Journal Cancer Biology & Therapy, 8, 1318–27. [PubMed: 19421008]

[21]. Liu L-Y, Man X-X, Yao H-X, Tan Y-Y. (2017) Effects of pheophorbide a-mediated photodynamic therapy on proliferation and metastasis of human prostate cancer cells. European Review for Medical and Pharmacological Sciences, 21, 5571–5579. [PubMed: 29271988]

[22]. Hagiya Y, Adachi T, Ogura S, An R, Tamura A, Nakagawa H, Okura I, Mochizuki T, Ishikawa T. (2008) Nrf2-dependent induction of human ABC transporter ABCG2 and heme oxygenase-1 in HepG2 cells by photoactivation of porphyrins: biochemical implications for cancer cell response to photodynamic therapy. Journal of Experimental Therapeutics and Oncology, 7, 153–67. [PubMed: 18771089]

[23]. Yang S-P, Wilson K, Kawa A, Raner G M. (2006) Effects of Green Tea Extracts on Gene Expression in HepG2 and Cal-27 Cells. Food and Chemical Toxicology, 44, 1075–1081. [PubMed: 16487642]
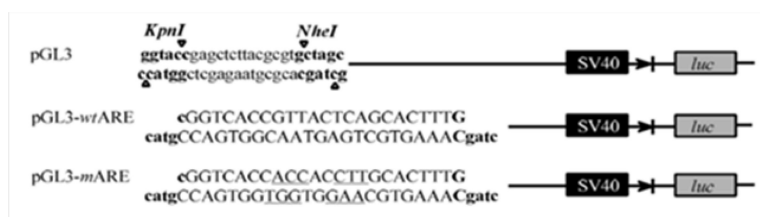
Figure 1:
Schematic illustration of promoter region of pGL3 plasmid vector, wild-type and mutant ARE constructs.
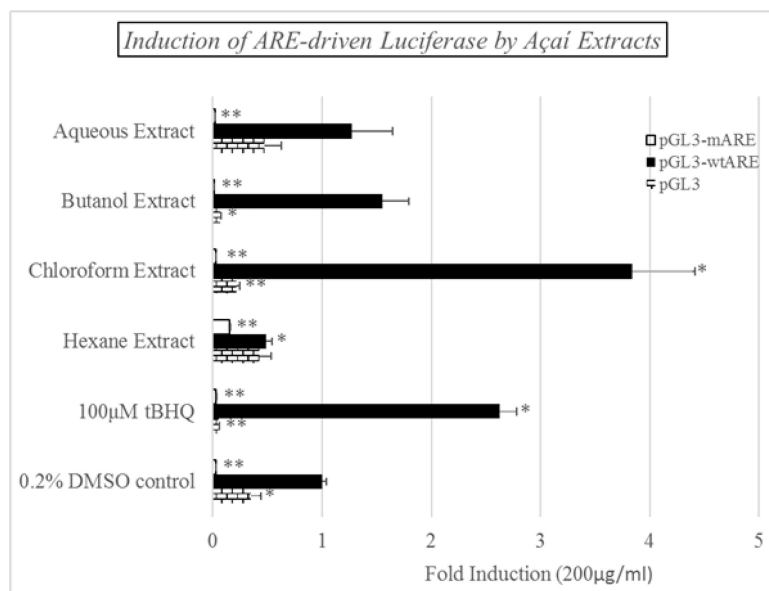
Figure 2:
Induction of ARE-driven luciferase expression in cultured HepG2 cells by the açaí-97-Series. The HepG2 cells were treated with each fraction at a dose of 50 μg/mL for 24 hrs.
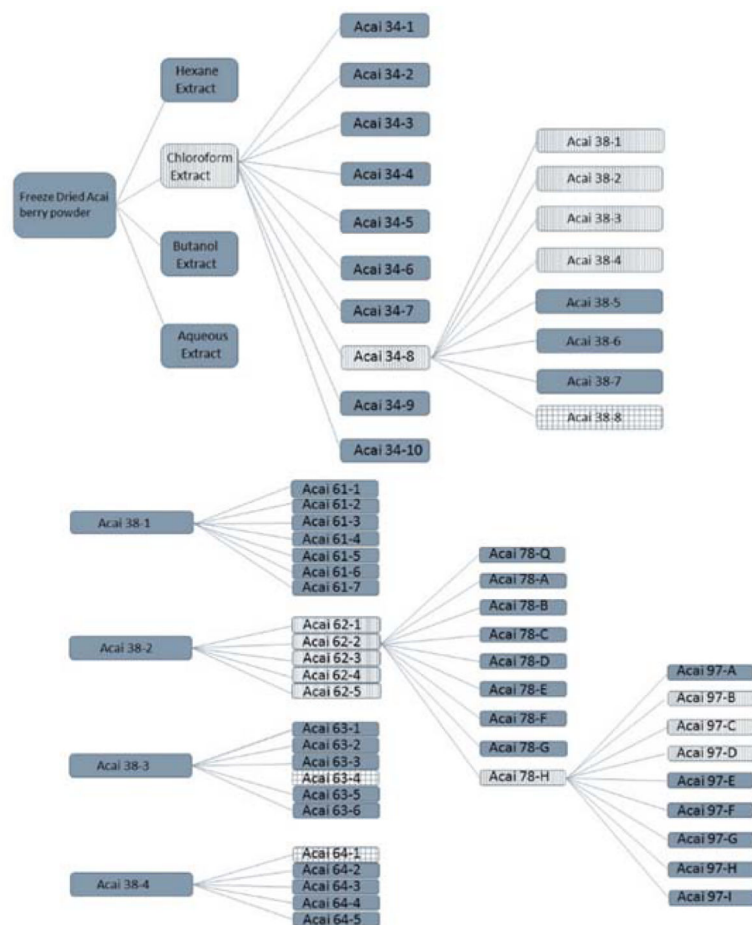
Figure 3:
Fractionation scheme for the active chloroform extract from açaí berry powder. The fractions highlighted with vertical lines were those selected for further fractionation in this scheme. The checkered fractions indicate those that were active but could not be further fractionated..
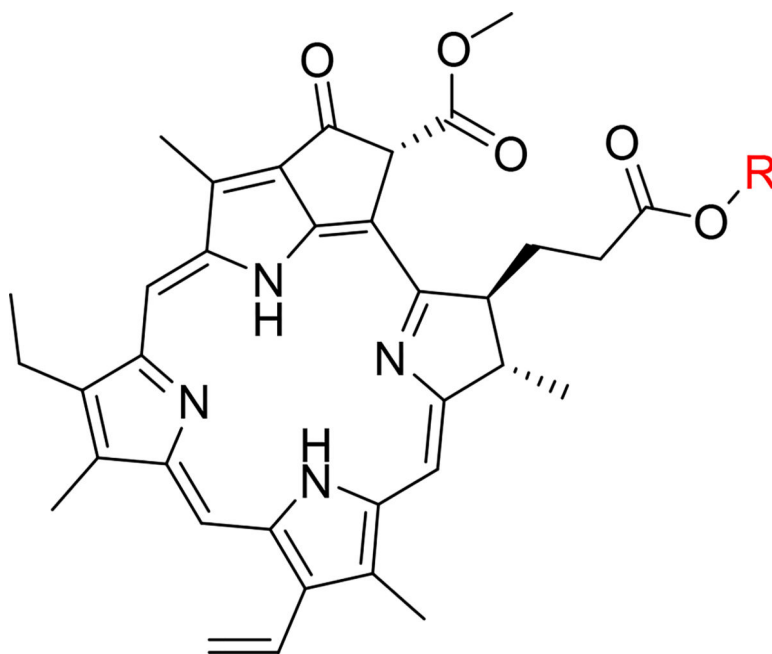
Figure 4:
General structure of the pheophorbide compounds isolated by activity guided fractionation. Açaí 97-B was identified as the methyl ester ($R=CH_3$) whereas Açaí 97-D was identified as the ethyl ester ($R=CH_2CH_3$).
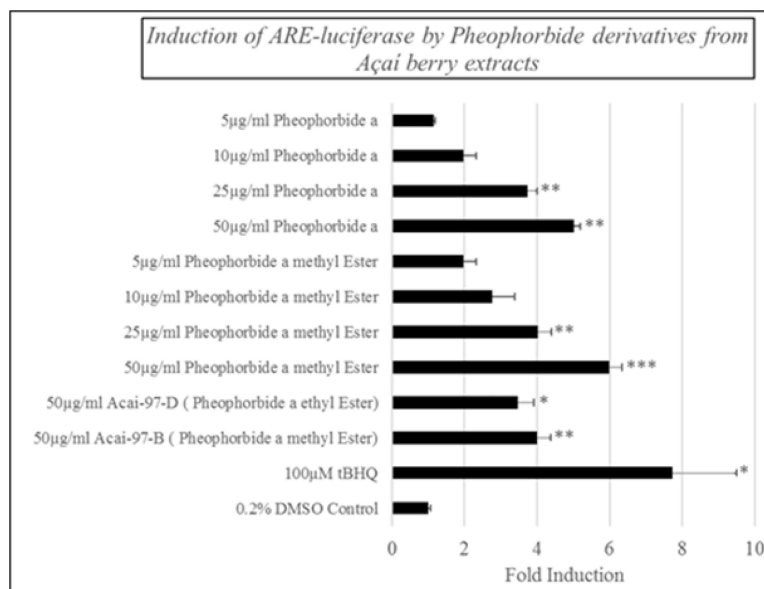
Figure 5.
Induction of ARE-driven luciferase expression in cultured HepG2 cells by pheophorbide a methyl ester and pheophorbide a. Cells were treated for 24 hrs at the indicated dose prior to measuring ARE-driven luciferase activity.